CHAPITRE 2 : Accumulation au sein des cellules endothéliales du cerveau d'anticorps monoclonaux ciblant le récepteur de la transferrine suite à une injection intraveineuse

Résumé

Le développement de vecteurs pour le ciblage thérapeutique au cerveau est encore aujourd'hui un enjeu pharmaceutique majeur. Dans cette étude, nous avons caractérisé la distribution cérébrale de différents anticorps monoclonaux (AcM) ciblant le récepteur de la transferrine (RTf) (clones Ri7 et 8D3) en comparaison avec un IgG témoin suite à une injection intraveineuse chez la souris. Les AcM ont été marqués avec des molécules fluorescentes de type Alexa Fluor™ (AF, AF647 ou AF750). L'injection systémique des AcM Ri7 et 8D3 marqués avec l'AF750 a engendré une augmentation de l'émission de la fluorescence sur des homogénats de cerveau en comparaison avec les AcM témoins indiquant une rétention au cerveau. Des analyses de microscopie en fluorescence ont démontré que le signal du Ri7-AF647 était confiné à la cérébrovasculature, suite à sa colocalisation avec un marqueur de la lame basale, le collagène IV. Des analyses plus poussées de microscopie confocale ont confirmé l'internalisation des AcMs Ri7 dans les cellules endothéliales du cerveau par l'utilisation du marqueur de péricytes contractiles *α-smooth muscle actin*, du marqueur endothélial CD31 et de l'anticorps collagène IV. Aucune colocalisation entre le signal du Ri7-AF647 et les neurones ou les astrocytes n'a été détectée en utilisant des marqueurs spécifiques pour le noyau neuronal ou le *glial fibrillary acidic protein*, respectivement. Nos résultats montrent que les vecteurs ciblant le RTf s'accumulent dans les cellules endothéliales du cerveau suggérant ainsi une nouvelle voie d'accès au cerveau pour le ciblage thérapeutique.

In vivo labeling of brain capillary endothelial cells after intravenous injection of monoclonal antibodies targeting the transferrin receptor

Sarah Paris-Robidas, Vincent Emond, Cyntia Tremblay, Denis Soulet, and Frédéric Calon

Faculty of Pharmacy (S.P.R., V.E., C.T., F.C.)

Faculty of Medicine (D.S.), Laval University, Quebec, Canada

Centre Hospitalier de l'Université Laval Research Center, Quebec, Canada (S.P.R., V.E., C.T., D.S., F.C.)

Running title: Vectors Targeting of Brain Capillaries

Corresponding author:

Frédéric Calon
Centre de recherche du CHU de Québec
Pav. CHUL, Room T267, 2705 Laurier Blvd,
Quebec (QC) G1V 4G2, Canada.
Email: frederic.calon@crchul.ulaval.ca

ABBREVIATIONS: BCEC, brain capillary endothelial cell; α-SMA, α-smooth muscle actin; AF, Alexa Fluor; BBB, blood-brain barrier; CNS, central nervous system; DAPI, 4,6-diamidino-2-phenylindole; GFAP, glial fibrillary acidic protein; MAb, monoclonal antibody; MMCO, molecular mass cutoff; NeuN, neuronal nuclei; PBS, phosphate-buffered saline; PFA, paraformaldehyde; Ri7, cell line Ri7217.1.4; TBS, Tris-buffered saline; TfR, transferrin receptor; RT, room temperature.

Abstract

The development of vectors for drug delivery to the central nervous system remains a major pharmaceutical challenge. Here, we have characterized the brain distribution of two monoclonal antibodies (MAbs) targeting the mouse transferrin receptor (TfR) (clones Ri7 and 8D3) compared with control IgGs after intravenous injection into mice. MAbs were fluorolabeled with either Alexa Fluor (AF) dyes 647 or 750. Intravenous injection of Ri7 or 8D3 MAb coupled with AF750 led to higher fluorescence emission in brain homogenates compared with control IgGs, indicating retention in the brain. Fluorescence microscopy analysis revealed that AF647-Ri7 signal was confined to brain cerebrovasculature, colocalizing with an antibody against collagen IV, a marker of basal lamina. Confocal microscopy analysis confirmed the delivery of injected Ri7 MAb into brain endothelial cells using the pericyte marker anti-smooth muscle actin, the endothelial marker CD31, and the collagen IV antibody. No evidence of colocalization was detected with neurons or astrocytes identified using antibodies specific for neuronal nuclei or glial fibrillary acidic protein, respectively. Our data show that anti-TfR vectors injected intravenously readily accumulate into brain capillary endothelial cells, thus displaying strong drug-targeting potential.

Introduction

The majority of synthetic drugs and virtually all biopharmaceuticals fail to cross brain capillary endothelial cells (BCECs) forming the blood-brain barrier (BBB), hindering the development of new pharmacotherapeutic strategies for central nervous system (CNS) diseases (Pardridge 2007c). A few potential BBB vectors targeting transport systems located in BCECs have been identified in the last 25 years, yet their subsequent development has not been translated into clinical applications (Gabathuler 2010).

Evidence for BCEC targeting and subsequent brain transport *in vivo* have been published with peptide vectors (Kumar et al. 2007, Demeule et al. 2008b, Hervé et al. 2008) low-density lipoprotein receptor (Pan et al. 2004), transferring (Skarlatos et al. 1995), and melanotransferrin (Demeule et al. 2002, Karkan et al. 2008). However, the most numerous data were obtained with monoclonal antibodies (MAbs) targeting the insulin (Coloma et al. 2000, Zhang et al. 2003c) or transferrin receptors (TfR) (Friden et al. 1991, Pardridge et al. 1994, Shi et al. 2000, Zhang et al. 2003b). These two receptors represent attractive targets because they populate BCECs throughout the BBB (Mash et al. 1990, Moos 1996, Kissel et al. 1998), where they are expected to carry their bloodborne substrates into the brain through receptor-mediated transcytosis (Pardridge et al. 1987, Qian et al. 2002, Pardridge 2007c).

The first study targeting the TfR *in vivo* was performed in the rat and reported direct binding to BCECs after systemic injection of a mouse MAb raised against the rat TfR (clone OX-26) (Jefferies et al. 1984). A few years later, the presence of radiolabeled OX-26 in a capillary-depleted fraction of brain homogenates was considered as evidence of penetration into brain parenchyma (Friden et al. 1991, Pardridge et al. 1991). In parallel, electron microscopy studies have shown internalization within rat BCECs of immunogold-labeled OX-26 perfused into the internal carotid (Bickel et al. 1994) or systemic injection of horseradish peroxidase-labeled OX-26 (Broadwell et al. 1996). Although it has been assumed from many studies that MAbs targeting rodent TfR undergo receptor-mediated transcytosis into the brain (Friden et al. 1991, Pardridge et al. 1994, Lee et al. 2000, Shi et al. 2000, Qian et al. 2002, Zhang et al. 2003b), direct evidence is scarce. Indeed, most reports use indirect outcome measures such as protein expression or enzymatic activity to conclude on vector transport (Shi et al. 2000, Zhang et al. 2003b, Kumar et al. 2007). Studies systematically examining the brain

penetration of OX-26 using radiolabel- ing and immunohistochemical approaches concluded that OX-26 is transported into BCECs, without actually crossing the BBB (Moos et al. 2001, Gosk et al. 2004).

The coupling of therapeutic drugs or gene medicine to vectors delivered into the CNS could have a dramatic impact in the pharmaceutical care of many diseases. To elucidate the transport of MAbs targeting the mouse TfR into BCECs or across the BBB, we have investigated the brain distribution of fluorolabeled Ri7 compared with 8D3 and control IgGs after intravenous administration.

Materials and Methods

Production and purification of MAbs in vitro

Hybridoma cell lines were cultured in CELLine bioreactors in MAb serum-free medium (BD Biosciences, Mississauga, ON, Canada). Supernatants were harvested weekly. MAbs were purified using HiTrap protein G columns and the Akta Prime Plus system (GE Healthcare, Baie d'Urfé, QC, Canada) according to the manufacturer's recommendations. Purified antibodies were concentrated with Amicon (Millipore Corporation, Billerica, MA) ultracentrifugal devices [molecular mass cutoff (MMCO), 30 kDa] and subsequently dialyzed against 0.01 M phosphate-buffered saline (PBS), pH 7.4, using slide-a-lyser dialysis cassettes (MMCO, 10 kDa; Pierce Chemical, Rockford, IL). Protein concentrations were determined using bicinchoninic acid assays (Pierce Chemical). Weekly yield of purified MAbs averaged 3 mg. Hybridoma cell lines Ri7217.1.4 (Ri7) and 8D3 secreting the rat MAbs specific for the mouse transferrin receptor (TfR) were, respectively, obtained from Drs. Jayne Lesley (Salk Institute, via Dr. Pauline Johnson at the University of British Columbia, Vancouver, BC, Canada) and Britta Engelhardt (University of Bern, Bern, Switzerland). Because Ri7 and 8D3 MAb led to similar results on homogenate and immunohistochemical analyses (Figs. 1 and 5), we focused on Ri7 for most experiments, because the hybridoma-based production of Ri7 was more cost-efficient in our hands.

MAb conjugation to alexa fluor dyes

MAbs (Ri7, 8D3, Ctrl IgG) (300 µg) were thiolated with a 40:1 M excess of freshly prepared 2-iminothiolane (Traut's reagent) after a 1-h incubation in 0.05 M sodium borate/0.1 mM EDTA, pH 8.5. Thiolated MAbs were diluted in 0.05M HEPES/0.1 mM EDTA, pH 7.0, and then concentrated using a Vivaspin (Sartorius Stedim Biotech, Aubagne, France) filter device (MMCO, 30 kDa). This step was repeated twice to discard 2-iminothiolane, to transfer MAbs into HEPES-EDTA buffer, and to reduce the final volume of the solution to less than 40 µl. To conjugate thiolated MAbs to Alexa Fluor (AF) dyes, 125 nmol concentration of the AF maleimide (Invitrogen, Carlsbad, CA) was added and incubated overnight in 2-ml glass bottles under inert nitrogen atmosphere. Two types of AF maleimide were used: AF750 C5-maleimide, and AF647 C2-maleimide. Vivaspin devices were then used to discard unbound AF maleimide and concentrate AF-conjugated MAbs. Volumes were completed to 200 µl with HEPES-EDTA buffer before intravenous injection.

Animals

Adult male BALB/c mice (Charles River Laboratories Inc., Wilmington, MA) weighing 20 to 30 g were used. They had free access to food and water. All procedures were performed in accordance with the Canadian Council on Animal Care standards and were approved by the animal ethics committee of the Centre Hospitalier de l'Université Laval.

Tissue preparation for postmortem analysis

One, 4, or 20 h after intravenous (caudal vein) injection of 300 µg of AF-conjugated antibodies, animals were sacrificed by terminal intracardiac perfusion under deep anesthesia with ketamine/xylazine. For competition studies, 1200 µg of unlabeled Ri7 were injected 1 h before AF750-Ri7 injection. Poorly perfused animals as assessed by the presence of blood in the brain were excluded from further analysis. For fluorescence quantification in brain homogenates, terminal perfusions were performed with approximately 25 ml of phosphate-buffered saline (0.1 M PBS). For studies on homogenates or goat anti-rat immunohistochemistry, brain extracts were snap-frozen in 2-methylbutane and stored at 80°C. For immunofluorescence experiments, 4% paraformaldehyde (PFA) was added to the perfusion buffer. Hemi- spheres were then postfixed in 4% PFA for 6 h and transferred to a 20% sucrose/0.5% sodium azide solution for cryoprotection. Coronal brain sections of 20 to 35 µm (free-floating immunofluorescence) and 12 µm (frozen immunohistochemistry) were, respectively, cut with a freezing microtome and a cryostat (Leica Microsystems, Richmond Hill, ON, Canada). Experiments were performed on between three and nine animals per group and on at least five sections per animals.

Brain homogenates

Brain extracts from mice injected with AF750-MAbs were homogenized in 4 volumes of Tris-buffered saline (TBS) containing the Complete protease inhibitor cocktail (Roche Diagnostics, Indianapolis, IN) and 10 µl/ml pepstatin A along with phosphatase inhibitors (50 mM sodium fluoride and 1 mM sodium pyrophosphate). Samples were sonicated briefly (3 x 10 s) and centrifuged at 100,000 xg for 20 min at 4°C to generate a TBS-soluble fraction containing intracellular and extracellular proteins (TBS-soluble fraction). The TBS-insoluble pellet was sonicated in 4 volumes of lysis buffer (150 mM NaCl, 10 mM NaH_2PO_4, 1% Triton X-100, 0.5% SDS, and 0.5% deoxycholate) containing the same

protease and phosphatase inhibitor cocktail. The resulting homogenate was centrifuged at 100,000g for 20 min at 4°C to produce a lysis buffer-soluble fraction (detergent-soluble fraction). The protein concentration in each fraction was determined using bicinchoninic acid assays. Samples were added to a black 96-well plate, and fluorescence was measured with a Kodak 4000MM image station with appropriate filters (excitation, 720 nm; emission, 790 nm). Images were analyzed and pseudocolored with the Kodak MI software (Carestream Health, Woodbridge, CT).

Immunohistofluorescence

Washes in 0.1 M PBS, pH 7.4, were performed between each steps of the immunohistofluorescence and immunohistochemistry (see below) protocols. Free-floating brain sections from mice injected with AF647-MAbs or unlabeled MAbs were blocked for 1 h in a PBS solution containing 5% horse serum (Invitrogen) and 0.2% Triton X-100. Sections were then incubated overnight at 4°C with primary antibodies in the blocking solution: goat anti-type IV collagen (1:500; Millipore Bioscience Research Reagents, Temecula, CA), mouse anti-neuronal nuclei (NeuN, 1:100; Millipore Bioscience Research Reagents), mouse anti-glial fibrillary acidic protein (GFAP, 1:100; Sigma-Aldrich, St. Louis, MO), and mouse anti-α-smooth muscle actin (α-SMA, 1:200; Calbiochem, San Diego, CA). After incubation with primary antibodies, slices were exposed to AF-conjugated donkey anti-goat and anti-mouse secondary antibodies (1:1000; Invitrogen, Carlsbad, CA). In some experiments, appropriate AF-conjugated secondary antibodies [donkey anti-rat (Ri7) or donkey anti-mouse (control IgG)] (1:1000; Invitrogen) were also used to detect MAbs administered intravenously. Sections were transferred onto SuperFrost Plus slides (Thermo Fisher Scientific, Waltham, MA) and placed under coverslips with Mowiol mounting media. To compare the signal in blood vessels versus brain parenchyma, fluorescence on brain section, images was analyzed with the Kodak MI software (Carestream Health, Rochester, NY).

Goat anti-rat and anti-mouse immunohistochemistry

Frozen brain slices (12 µm) from mice injected with unlabeled MAbs were cryostat-sectioned onto SuperFrost Plus slides, desiccated at 4°C, and immersed in 3% peroxide for 30 min at RT. Slides were then incubated in a blocking and permeabilizing PBS solution containing 0.2% Triton X-100 (Sigma-Aldrich) and 5% horse serum (Invitrogen) for 30 min at RT. To detect previously injected Ri7 and control IgG MAbs, which thus served as primary antibodies, sections were incubated in the

blocking buffer with 1:1500 biotinylated goat anti-rat or goat anti-mouse antibodies (Jackson ImmunoResearch Laboratories Inc., West Grove, PA). Slides were then placed in ABC solution of avidin-peroxidase (ABC Elite Kit; Vector Laboratories, Burlington, ON, Canada) for 1 h at RT and incubated with 3-amino-9-ethylcarbazole solution (Sigma-Aldrich) for 20 min. Finally, sections were exposed to Gill No. 2 hematoxylin solution (Sigma-Aldrich) for 30 s and placed under coverslips with Mowiol mounting media.

Brain localization of TfR

Frozen brain slices (12 μm) from untreated (control) mice were cryostat-sectioned onto SuperFrost Plus slides (Thermo Fisher Scientific) and desiccated at 4°C. After- ward, slides were immersed in 4% PFA at RT and incubated in a blocking PBS solution containing 0.2% Triton X-100 (Sigma-Aldrich) and 5% horse serum (Invitrogen) for 1 h at RT. Sections were then incubated in the blocking buffer with rat Ri7 (anti-TfR, described previously; concentration, 18.5 mg/ml, 1:500), used as a primary antibody, mouse anti-NeuN (1:1000; Millipore Bioscience Research Reagents), and goat anti-type IV collagen (1:500; Millipore Biosci- ence Research Reagents) overnight at 4°C. After incubation, slides were revealed with AF-conjugated donkey anti-rat, anti-mouse, and anti-goat secondary antibodies (1:1000; Invitrogen). Sections were subsequently treated with 0.5% Sudan Black (in 70% methanol) for 5 min and placed under coverslips with Mowiol mounting media.

Confocal microscopy and 3D reconstruction of brain blood vessels

Free-floating 35 μm brain sections from mice injected with AF647-MAbs were blocked for 1 h in 0.1 M PBS, 5% horse serum and 0.2% Triton X-100. Slices were then incubated with a goat anti-type IV collagen antibody (1:500) overnight at 4°C in the blocking solution. Afterward, sections were incubated with a biotinylated rabbit anti-goat antibody (1:1000) for 2 h at RT followed by AF546- conjugated streptavidin (Invitrogen, 1:1000) for another 2 h at RT. To block rat Ri7 and prevent subsequent detection by anti-rat secondary antibodies, slices were then incubated with a goat anti-rat monovalent antibody (fragment antigen-binding fragment, 1:250; Jackson Immunoresearch Laboratories) for 2 h at RT. Afterward, sections were incubated with rat anti-CD31 (1:1000; Biolegend, San Diego, CA) overnight at 4°C and then incubated with a donkey anti-rat AF488 secondary antibody (Invitrogen, 1:1000), for 2 h at RT. Finally, slices were counterstained with 4,6- diamino-2-phenylindole (DAPI; Invitrogen), mounted on SuperFrost Plus slides, treated with 0.5%

Sudan black (in 70% methanol) for 5 min, and placed under coverslips with Mowiol mounting media. Confocal laser scanning microscopy was performed with a BX-61 microscope equipped with the Fluoview FV500 imaging software 4.3 (Olympus America Inc., Melville, NY). Confocal images were acquired by sequential scanning using a three-frame Kalman filter and a z-step of 0.25 m. Stacks were restored by blind deconvolution using SVI Huygens Suite 2.7 software, and then the image pseudo-colors were adjusted to enhance contrast. Maximum intensity projections and volume rendering were calculated using the Surpass module in Imaris 4.1 (Bitplane Inc., Zurich, Switzerland). Video was encoded by Apple Keynote '09 (Apple Computer, Cupertino, CA). To quantify the relative intensity of fluorescent signals, the "plot profile" function of ImageJ 1.43m (Wayne Rasband, National Institutes of Health, Bethesda, MD; http://rsbweb.nih.gov/ij/) was applied to the line in Supplemental Fig. S2. Fluorescence values were expressed as an arbitrary unit. Colocalization analysis was performed in Imaris 4.1 (Bitplane Inc.) using the Costes' estimation of automatic threshold, which compares the Pearson's coefficient for nonrandomized versus randomized images and calculates the significance (Costes et al. 2004). Colocalization channels of Ri7 in CD31 and Ri7 in collagen IV were generated for visual representation, and Pearson's coefficients were calculated.

Statistical analysis

Two-sided Student's unpaired t tests were used to detect significant differences between two groups when appropriate. Welch correction was used when variances were different between groups. Statistical significance was set at * $p < 0.05$, ** $p < 0.01$, and *** $p < 0.001$. All statistical analyses were performed using Prism 4 for Macintosh (GraphPad Software Inc., San Diego, CA).

Results

Fluorescent anti-TfR MAbs accumulate in brain homogenates after intravenous injection

To gather a first overview of the distribution of AF750-labeled Ri7, 8D3, and Ctrl IgG, fluorescence in brain homogenates was measured 1 h after intravenous injection. Higher fluorescence was detected in brain homogenates from animals injected with the two antibodies targeting the mouse TfR (Ri7 and 8D3) compared with mice injected with control IgGs (Figure 13A). The three control IgGs led to a comparable low signal, whereas both Ri7 and 8D3 MAbs gave an equivalent, high fluorescence signal (Figure 13A). Quantification and statistical comparison on groups of animal [Ri7 (n 8), control IgG (n 8), Ri7(C) (n 4)] confirmed the significant accumulation of Ri7 in whole brain homogenates compared with control IgG (Figure 13B). Moreover, preinjecting a four-time excess of unlabeled Ri7 prevented the accumulation of AF750-Ri7 in brain tissue (Figure 13B). A separate experiment confirmed that AF750-Ri7 signal 24 h after intravenous injection remained at approximately 50% of the value obtained after 1 h. The increase of fluorescence was particularly striking in the detergent-soluble fractions of brain homogenates, consistent with the entrapment of the AF750-Ri7-TfR complex into membrane compartments.

Injection of Fluorolabeled Anti-TfR MAbs targets brain microvessels

The detection of fluorescence emission from blood-free brain homogenates did not discriminate between Ri7 localized within BCECs, large vessels, brain parenchyma (neurons and glial cells), cerebrospinal fluid or meninges. To determine the brain distribution of TfR-targeting vectors at a microscopic level, we conducted fluorescence microscopy analysis after intravenous injection of AF647-Ri7, in at least 3 animals per experimental group. The representative example shown in Figure 14A indicate that the signal associated with AF647-Ri7 injected intravenously was confined to the cerebral microvasculature and was strong after 1 and 4 h but had declined after 20 h. Colocalization with small (>10 μm) and large (<10 μm) blood vessels was validated using an anti-collagen IV antibody, a marker of basal lamina surrounding brain microvessels, including BCECs (Figure 14B). Image analysis of 10 sections per animals confirmed that virtually 100% of the fluorescence signal was localized within microvessels.

Next, to determine whether AF647-Ri7 reached neurons, colocalization analyses with NeuN antibody to label neuron nuclei were performed. In at least nine different animals injected with fluorolabeled Ri7, we did not observe a single convincing example of signal within a neuron, as shown in Figure 15A. Likewise, no evidence of colocalization with GFAP-labeled astrocytes was observed (Figure 15B). Similar data were obtained with AF568-8D3 (Supplemental Figure S1).

To rule out the possibility that a very low expression of TfR on neurons explains our results, we conducted an immunohistofluorescence experiment on brain sections from a mouse. We show in Figure S2 that AF488-coupled Ri7 binds to both collagen IV-labeled microvessels and NeuN-stained neurons, confirming earlier reports (Jefferies et al. 1984, Markelonis et al. 1988, Giometto et al. 1990, Moos 1995). Thus, massive penetration of systemically injected Ri7 within brain parenchyma would have been expected to immunolabel neurons as well.

The data accumulated so far clearly showed that AF647- Ri7 labeled vessels with a diameter of less than 10 μm, indicating that AF647-Ri7 bound to brain capillaries. To further validate that injected Ri7-labeled BCECs and not just large arterioles, we performed smooth muscle actin (α-SMA) immunolabeling experiments on sections from four animals injected with AF647-Ri7 and four animals injected with AF647-IgG. Because pericytes expressing α-SMA are more rarely found around capillaries, α-SMA immunolabeling is often used to distinguish arteries/arterioles from capillaries (Dore-Duffy & Cleary 2011). We consistently found that numerous pericytes were indeed found around large vessels, but less frequently distributed in capillaries in which AF647-Ri7 labeling was abundant, thus further confirming that the Ri7 vector actually reached BCECs (Figure 16).

To determine whether coupling to the AF dye in previous experiments altered the capacity of Ri7 to be cargoed into brain parenchyma, we injected unlabeled Ri7 and conducted immunohistochemistry and immunofluorescence experiments using anti-rat secondary antibodies. Consistent with data obtained with AF-coupled vectors, systemic injection of rat antibody Ri7 or 8D3 led to the specific immunostaining of BCECs in comparison with a control MAb (Figure 17A). Once again, no indication of colocalization with NeuN-labeled neurons or GFAP-labeled astrocytes was detected (Figure 17, B and C).

Fluorolabeled anti-TfR MAbs reached all subcellular compartments of BCECs

Confocal microscopy was used to assess whether anti-TfR AF647-MAbs were internalized by BCECs or remained at their luminal surface. We observed that fluorescence from AF647-Ri7 targeting the murine TfR colocalized with an endothelial cell marker (CD31 or platelet endothelial cell adhesion molecule) and with type IV collagen, a marker of the basal lamina (Figure 18). Fluorolabeling of the basal lamina and BCECs allowed us to delimit more precisely the localization of Ri7 MAbs (Supplemental Figure S3). Evidence of colocalization was supported by the results of Pearson's coefficients after the statistical approach of Costes' colocalization method (Costes et al. 2004). The Pearson's coefficient was 0.42 in the colocalized volume of Ri7 with CD31 and 0.07 in the colocalized volume of Ri7 with type IV collagen. Therefore, the Ri7 MAb was significantly colocalized with BCECs but also reached the basal lamina, although to a lesser extent. Furthermore, animated three-dimensional reconstructions of brain microvessels provide additional visual support that intravenously injected AF647-Ri7 MAbs were internalized by brain endothelial cells (Supplemental Movie S1).

Discussion

In the present work, we have characterized the brain distribution of systemically administered fluorolabeled MAbs targeting the mouse TfR. Using different antibodies, fluorescent dyes and technical approaches, our results clearly indicate that anti-TfR MAbs Ri7 and 8D3 specifically bind to TfR located on BCECs.

Using brain homogenates, the results of our first series of experiments are consistent with the hypothesis that fluorolabeled anti-TfR MAbs Ri7 and 8D3 were uptaken by the brain after intravenous injection. These observations are in accordance with previous studies with anti-TfR antibodies such as tritiated Ri7 and 8D3 in mice (Lee et al. 2000) or tritiated OX-26 in rats (Friden et al. 1991, Pardridge et al. 1991, Moos et al. 2001). The absence of penetration of the three control IgGs used here and the competition by unlabeled Ri7 confirmed that specific binding to the mouse TfR was required. However, no conclusion on whether the vectors actually crossed the BBB could be reached because BCECs were included in brain homogenates.

Our subsequent microscopic analysis clearly showed that injecting Ri7 into the bloodstream specifically labeled brain microvessels, an interpretation further supported by colocalization analyses with a collagen IV antibody. Colocalization analysis with pericytes further confirmed that intravenously injected AF647-Ri7 bound to TfR located on capillaries (i.e., BCECs). In addition to brain endothelial cells, TfRs are also found on the plasma membrane of neurons (Jefferies et al. 1984, Markelonis et al. 1988, Giometto et al. 1990, Moos 1995), as confirmed here in Supplementary Fig. S2, and on reactive astrocytes (Orita et al. 1990). It can thus be proposed that systemically administered anti-TfR MAbs could be further carried into neurons and astrocytes as well (Pardridge 2007c). However, our studies at a microscopic level rather indicated that the distribution of anti-TfR antibodies injected in the bloodstream was limited to BCECs. This is in agreement with the immunohistochemical work of Moos and colleagues, using anti-TfR antibody OX-26 in the rat brain (Moos et al. 2001, Gosk et al. 2004). A previous electron microscopy-based report has also shown the accumulation of blood-borne horseradish peroxidase-labeled OX26 into BCECs, but the experiments in this study did not include controls (Broadwell et al. 1996).

The present investigations do not provide evidence for quantitatively significant brain uptake of anti-TfR antibodies farther than BCECs. One possible explanation of the absence of signal in neurons

would be that the coupling of large AF moiety to MAb vectors might have hindered its BBB transport. However, separate immunohistochemistry experiments after injection of unlabeled Ri7 confirmed its specific distribution in BCECs. Nonetheless, the present data do not rule out the possibility that anti-TfRs are transported in limited amount across the BBB and into the brain parenchyma. It remains a possibility that the sensitivity of the approach was not sufficient to detect the presence of Ri7 outside of BCECs, in which case, small amounts of Ri7 signal in neurons or other brain cells may have gone undetected. Electron microscopy could provide the sensitivity needed to detect small amount of antibodies outside of the BCECs that might have reached the parenchyma. On the other hand, poorer stability of the fluorophore and/or vectors in neuron and astrocytes may explain the absence of signal in these types of cells. In this regard, it has been hypothesized that the transferrin-TfR complex undergoes endocytosis, releases its iron in the acidic environment of the endosome, and is then recycled back to the luminal membrane of BCECs (Moos et al. 2007). It is therefore possible that Ri7-MAbs follow the same fate, which would explain its retention into BCECs. However, it is also conceivable that Ri7 MAbs are eventually simply degraded because the strength of the Ri7-TfR bond is unlikely to be reinforced by the endosome pH, as is the case for the transferrin-TfR interaction. Nevertheless, for the purpose of using Ri7 as a neuron-targeting vector, a significant and easily detectable accumulation in the targeted cells would seem to be a necessary premise. Thus, our results do not lend support to the use of the anti-TfR antibody Ri7 as a neuron-targeting vector.

The addition of confocal quantitative analyses based on a statistical intensity correlation suggest that anti-TfR Ri7 MAbs were incorporated into brain endothelial cells rather than just remaining bound on their luminal side. Whereas electron microscope studies may help to definitively answer this question, the strong colocalization with CD31 provides compelling evidence of a wide distribution of Ri7 MAbs throughout brain endothelial cells. Furthermore, partial colocalization with collagen IV suggests that the vectors reached the basal lamina beyond the abluminal space (Figure 19).

Overall, our data strongly argue in favour of using anti-TfR Ri7 MAb as an effective BCEC-targeting vector. Such transport of anti-TfR vectors into BCECs can be extremely interesting from brain-targeting and therapeutic perspectives. Indeed, BCECs display secretory capacity and are widely distributed throughout the CNS in close proximity with neurons or glial cells. Vectorized gene therapy delivered into BCECs could thus be used to access CNS cells (Jiang et al. 2002, Jiang et al. 2003) or to target pathological processes specific to BCECs. In this regard, it has been proposed that

BCECs play critical roles in prevalent brain disorders such as neurodegenerative disease or stroke (Cirrito et al. 2005, Zlokovic 2008a, Deane et al. 2009, Weiss et al. 2009a). In summary, vector-driven incorporation of drugs into BCECs may thus hypothetically be tailored to exert a variety of therapeutic effects against CNS diseases.

In conclusion, MAbs targeting the TfR and other BBB transport systems are at the core of intense research endeavors aiming at developing vectors to enable drug delivery to the brain. The present study provides evidence that anti-TfR MAbs bind in massive amount to TfRs located on the cerebral vasculature, which opens the door to BCEC-based drug targeting opportunities into the CNS.

Authorship Contributions

Participated in research design: Calon.

Conducted experiments: Paris-Robidas, Emond, Tremblay, and Soulet.

Performed data analysis: Paris-Robidas, Emond, Soulet, and Calon.

Wrote or contributed to the writing of the manuscript: Paris-Robidas, Emond, Soulet, and Calon.

Other: Calon acquired funding for this research.
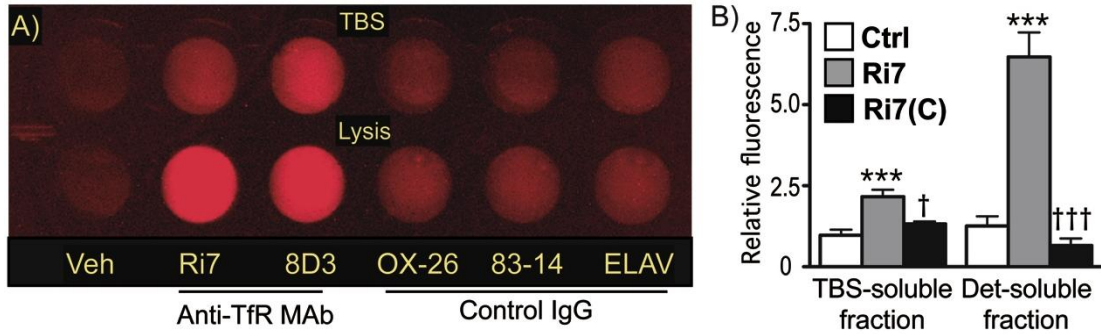
Figures

Figure 13: Brain accumulation of MAbs targeting murine TfR after an intravenous injection.

A, mice were injected with 300 µg of AF750-labeled MAbs targeting murine TfR (Ri7 and 8D3) or AF750-labeled control IgGs and were sacrificed by intracardiac perfusion 1 h later. A representative pseudocolored image of brain homogenate fractions is illustrated. B, quantification of fluorescence emission in brain homogenates of mice 1 h after intravenous injection of 300 µg of either control IgGs (Ctrl, n = 8), AF750-Ri7 (Ri7, n = 8), or AF750-Ri7 1 h after a preinjection of 1200 µg of unlabeled Ri7 [Ri7 (C), n = 4]. Data were normalized based on the degree of labeling of each MAb, and background values from saline-injected animals were subtracted from each measure. Data represented are means S.E.M. Statistical comparisons: one-way analysis of variance followed by a Tukey- Kramer post hoc test. ***, p 0.001 versus Ctrl IgG; †, p 0.05, and †††, p 0.001 versus Ri7. Det, detergent.
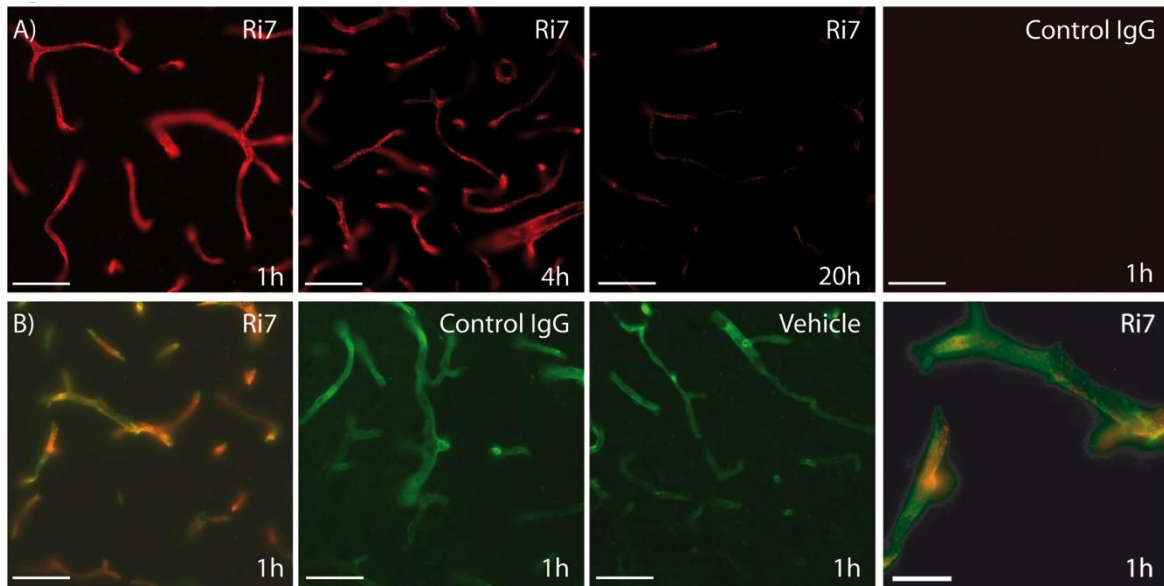
Figure 14: Labeling of BCECs after intravenous injection of MAbs targeting murine TfR.

Mice were injected with AF647-labeled MAbs targeting murine TfR (Ri7) or control IgG. Examples shown are typical from results repeated on three to nine animals. A, animals were sacrificed 1 (n = 9), 4 (n = 3), or 20 h (n = 3) after injection. Subsequent microscopic analysis showed that AF647 signal in red was present only in the brain of mice injected with MAbs targeting TfR (Ri7). The fluorescent signal was strong after 1 and 4 h but declined 20 h after the injections. Scale bars, 50 µm. B, AF647-Ri7 (red) colocalized with immunostaining of collagen IV on the basal lamina of BCECs (green), whereas no AF647 signal (red) was detected in animals injected with AF647-labeled control IgGs or vehicle. Scale bars are 50 µm, or 20 µm for the higher magnification image at the extreme right.
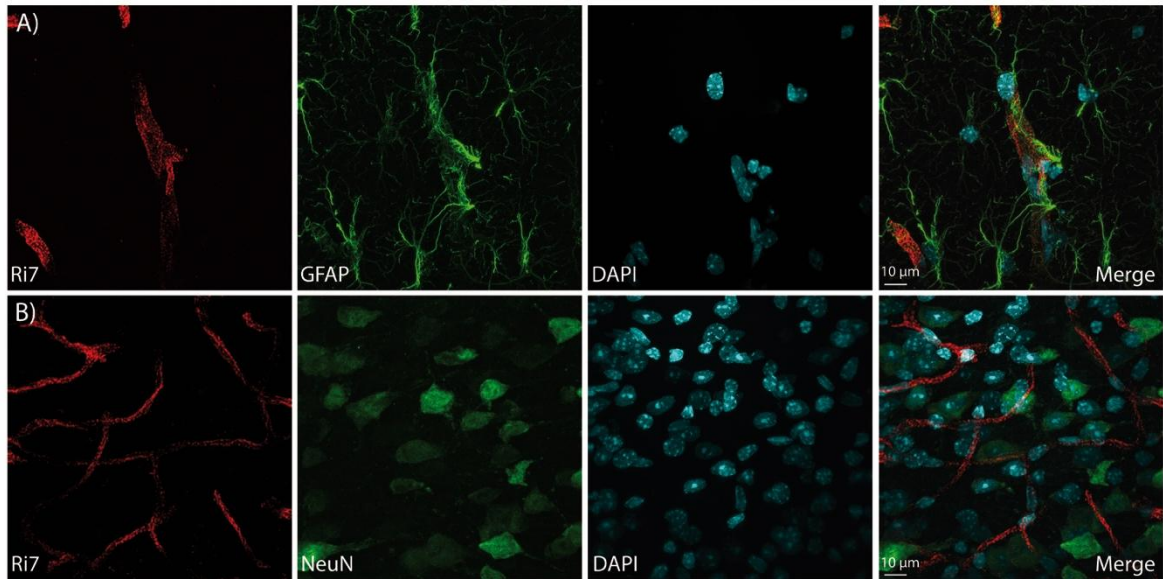
Figure 15: AF647-labeled Ri7 vectors were not detected in neurons or astrocytes after intravenous injection.
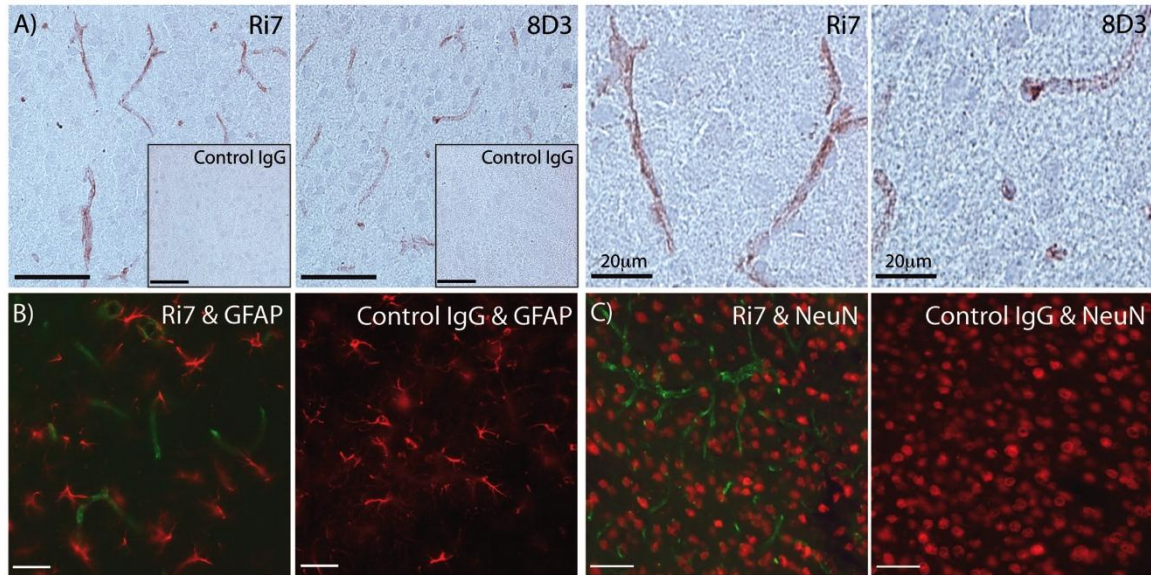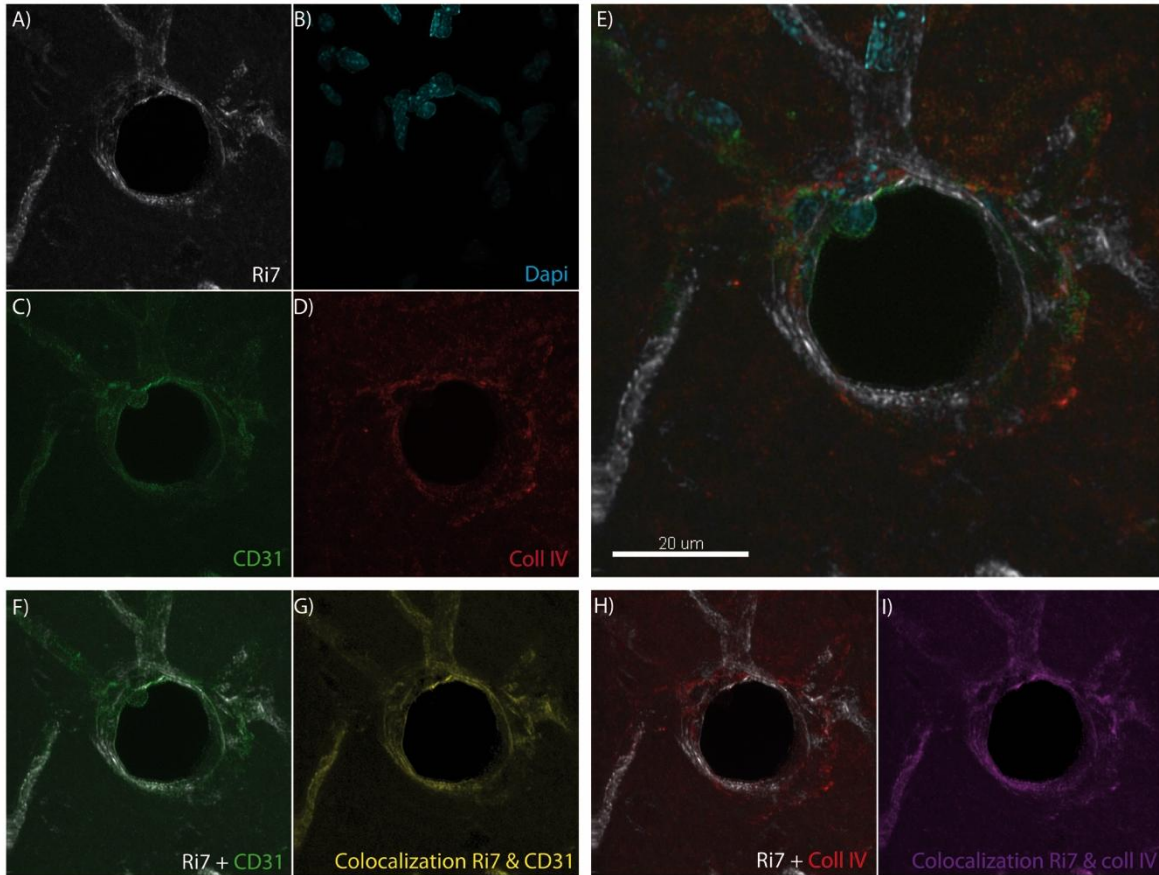
Mice were injected with AF647-labeled MAbs targeting the TfR (Ri7) (*n* = 9) and euthanized 1 h after the injection. A, AF647-labeled Ri7 (red) compared with neuronal marker NeuN (green). B, AF647-labeled MAbs Ri7 (red) with astrocyte marker GFAP (green). Scale bars for A and B, 10 µm.
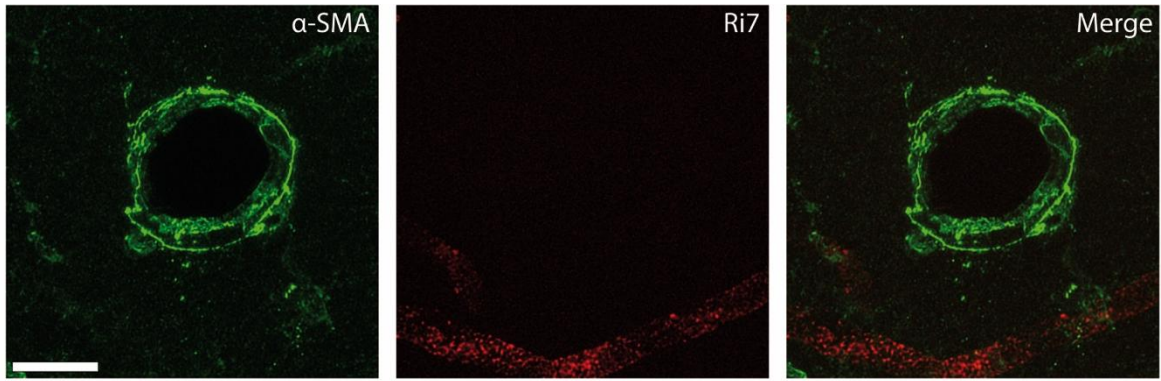
Figure 16: AF647-Ri7 labeling is more intense on small capillary than on a large microvessel surrounded by pericytes.

Mice were injected with AF647-labeled MAbs targeting the TfR (Ri7) (n = 4) and euthanized 1 h after the injection. The presence of AF647-labeled MAbs Ri7 (red) on a small capillary where pericytes identified with α-smooth muscle actin (green) are uncommon confirmed that Ri7 preferentially bind BCECs rather than the large blood vessel densely surrounded by pericytes. Scale bars, 20 µm.

Figure 17: The brain distribution of unlabeled Ri7 MAbs was restricted to brain microvessels after intravenous injection.

Mice were injected with unlabeled MAbs targeting TfR (Ri7) (*n* = 3), control IgG (*n* = 3), and vehicle (*n* = 3) and sacrificed 1 h after the injection. A, a representative example of immunohistochemistry using anti-rat secondary antibodies is shown, consistent with the specific binding of Ri7 MAbs to BCECs. B, using AF488-labeled anti-rat secondary antibodies, no colocalization of Ri7 MAb (green) with NeuN-labeled neurons (red) or (C) GFAP-positive cells (red) was observed. Scale bars, 20 μm unless indicated otherwise.

Figure 18: Evidence of internalization of anti-TfR MAbs within endothelial cells.
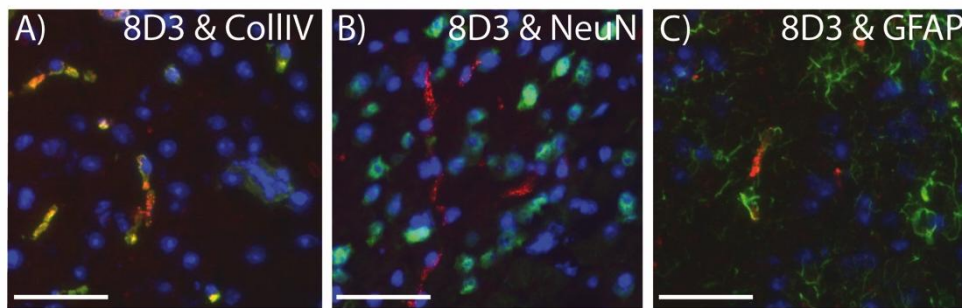
Mice were injected with AF647-labeled anti-TfR MAbs (Ri7) (*n* = 4) and were sacrificed 1 h after injection. A to D, representative confocal images showing immunolabeled brain microvessels with CD31 (green), DAPI (cyan), basal lamina marker collagen IV (red), and anti-TfR MAbs Ri7 (white) and merged together (E). The colocalization channel of CD31 in Ri7 (F) is shown in yellow (G), whereas the colocalization channel of collagen IV in Ri7 (H) was also calculated and represented in magenta (I). Scale bar, 20 µm. See Supplemental Movie S1 for three-dimensional reconstruction of this network of microvessels.
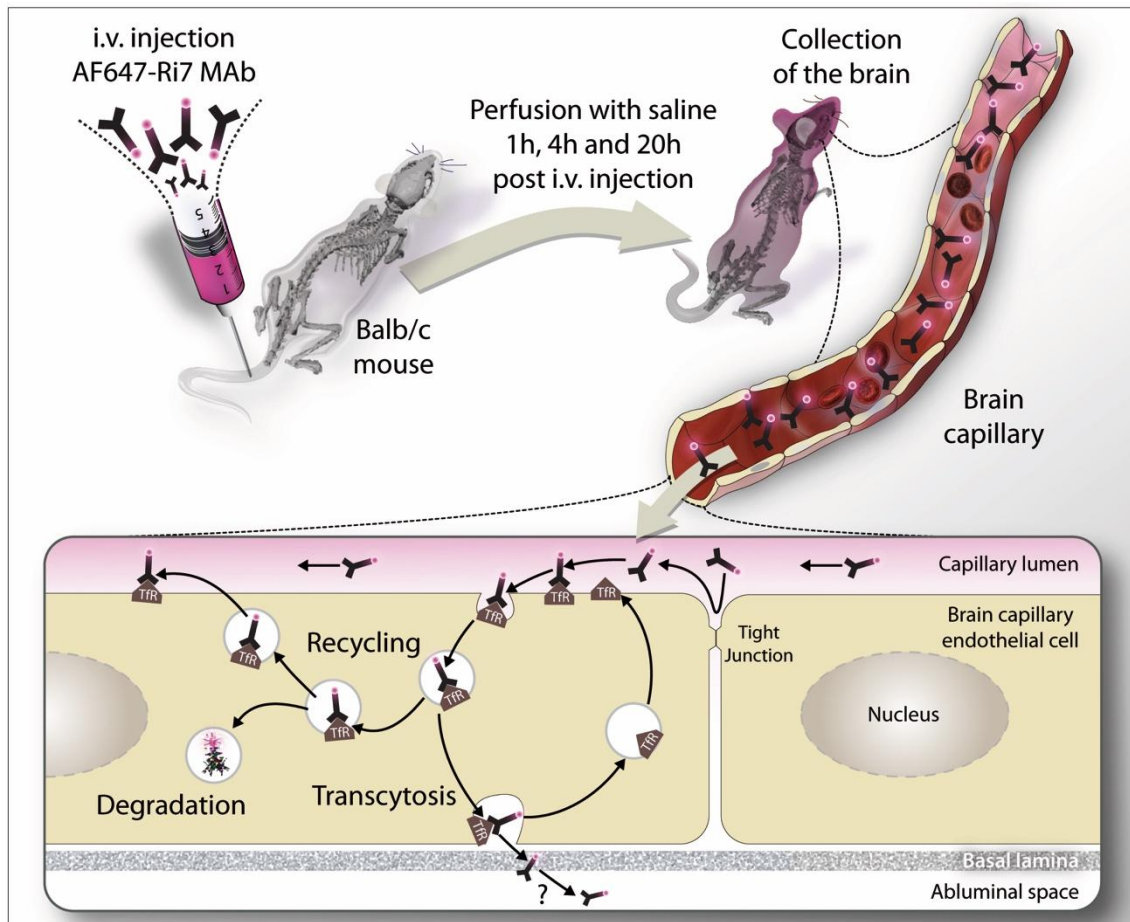
Figure 19: Model depicting potential mechanisms involved in the distribution of anti-TfR MAbs such as Ri7 in brain capillaries.

AF647-conjugated Ri7 MAbs injected intravenously in mouse are captured by BCECs through binding to the mouse TfR. Ri7 MAbs are then transported toward the basal lamina via transcytosis, in which they can potentially reach the abluminal space. On the other hand, Ri7 MAbs are degraded in the BCECs or transported back to the luminal membrane after the recycling of the TfRs.

Supplementary materials

Figure 20: Intravenously injected 8D3 MAbs specifically labeled brain microvessels after intravenous injection.

Mice were injected with AF568-labeled MAbs targeting the TfR (8D3) (n=3) and euthanized 1 h after the injection. (A) AF568-signal in red was present only in the brain of mice injected with 8D3 MAbs targeting TfR and restricted to microvessels identified using a collagen IV marker (green). No signal was detected with AF568-labeled control IgG. No evidence of colocalization outside microvessels was found using (B) neuronal marker NeuN (green) and (C) astrocytes marker GFAP (green). Nuclei were counterstained with DAPI (blue). Scale bar = 50 µm
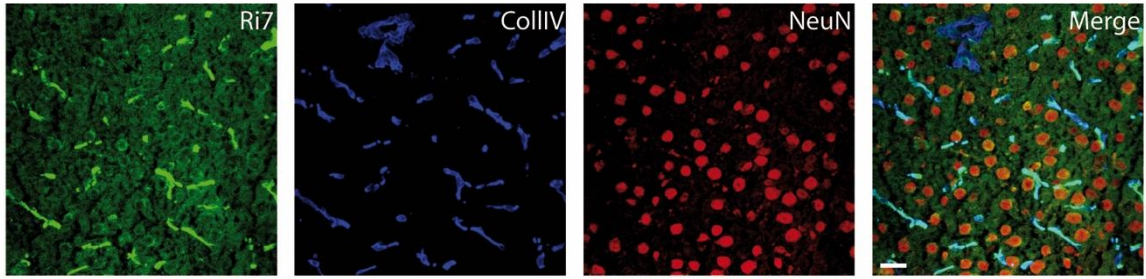
Figure 21 : Confirmation of the presence of TfR on both microvessels and neurons as measured with Ri7 immunohistofluorescence.

Confocal images showing representative results from two separate experiments of the localization of TfR (Ri7, green) on brain section from an untreated mouse (n=3), compared to basal lamina of microvessels (collagen IV, blue) and neurons (NeuN, red). The overlay image to the right shows that TfR are found on both microvessels and neurons. Scale bar = 30 μm.
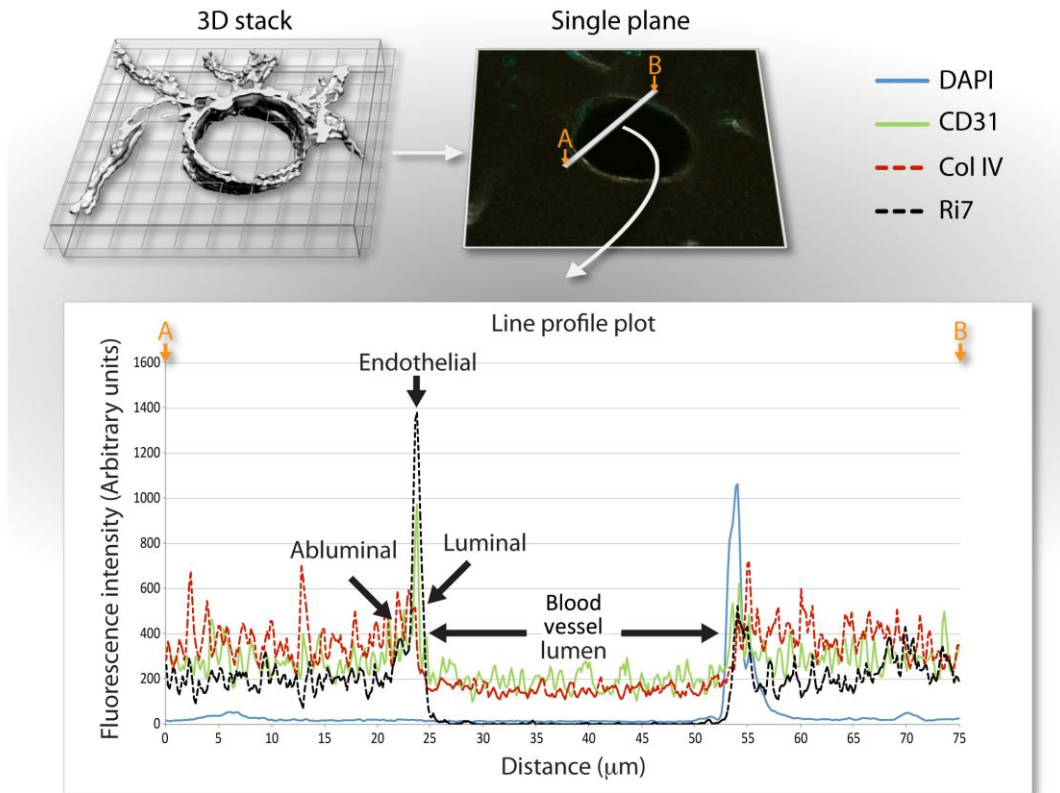
Figure 22: Line profile plot of the distribution of the anti-TfR MAb Ri7 suggests a luminal, endothelial, and abluminal distribution in brain microvessels.

Mice were injected intravenously with AF647-labeled anti-TfR MAbs (Ri7) and were sacrificed 1 h post-injection. Confocal images from brain microvessels immunolabeled with CD31 (green), DAPI (cyan), basal lamina marker collagen IV (red) and anti-TfR MAbs Ri7 (white) were acquired. Line profile analysis shows the distribution of fluorescence intensity of Ri7 labeling within the abluminal space (collagen IV) and the BCECs as well as the lumen of the capillary. Abbreviations: MAbs, monoclonal antibodies; TfR, transferrin receptor.